Quantum logic gates from time-dependent global magnetic field in a system with constant exchange

A. V. Nenashev,[1,2,*] A. F. Zinovieva,[1] A. V. Dvurechenskii,[1,2] A. Yu. Gornov,[3] and T. S. Zarodnyuk[3]

[1] *Rzhanov Institute of Semiconductor Physics SB RAS, 630090 Novosibirsk, Russia*
[2] *Novosibirsk State University, 630090 Novosibirsk, Russia*
[3] *Institute for System Dynamics and Control Theory SB RAS, 664033 Irkutsk, Russia*

(Dated: January 27, 2015)

We propose a method for implementation of an universal set of one- and two-quantum-bit gates for quantum computation in the system of two coupled electrons with constant non-diagonal exchange interaction. Suppression of the exchange interaction is offered to implement by all-the-time repetition of single spin rotations. Small g-factor difference of electrons allows to address qubits and to avoid strong magnetic field pulses. It is shown by means of numerical experiments that for implementation of one- and two-qubit operations it is sufficient to change the amplitude of the magnetic field within a few Gauss, introducing in a resonance one and then the other electron. To find the evolution of the two-qubit system, we use the algorithms of the optimal control theory.

PACS numbers: 73.21.La, 85.75.-d, 03.67.Lx

INTRODUCTION

There have been numerous proposals for implementation of quantum computation schemes in different material realizations, such as photon qubits, trapped atoms and ions, nuclear spins in molecules in liquid solutions, spin or charge states in quantum dots (QDs) or dopants in solids, and superconducting circuits [1]. Each such system must satisfy to 5 DiVinchenzo criteria: scalability, initialization ability, long coherence lifetime, universal set of quantum gates realization, readout ability [2]. Inspired by the Loss and DiVincenzo proposal [3], there is a continuing experimental effort to realize electron spin quantum bits or qubits in semiconductor quantum dots.[4] There, a single qubit is defined by the two spin states of an electron localized in a quantum dot (QD). Coupling between qubits is provided by exchange interaction between electrons in neighboring quantum dots. For single-qubit rotations the electron spin resonance (ESR) technique was proposed [5]. Two-qubit operations can be performed as combinations of the $\sqrt{SWAP}$ operation (based on the exchange interaction) with single-spin rotations. Read-out procedure can be realized via the spin-to-charge conversion [6]. In light of the foregoing, semiconductor QD systems are well suited for quantum computing, provided that the decoherence time in the system is long enough and there is a possibility of the system initialization. Realization of this proposal needs a system of electrodes. One type of electrodes provides the control of the exchange coupling during two-qubit operations, and the second type of electrodes allows to address an individual spin for one-qubit operations. In subsequent articles, the g-factor engineering or the local magnetic field gradient were proposed additionally for one-qubit operations [7, 8].

Two-qubit manipulation using electrical gates is actually quite a challenge. The complexity of this approach can be recognized by comparison of two following dates, the Loss and DiVincenzo proposal [3] has been published in 1998, while an experimental implementation of two-qubit operation in a double quantum dot has been made only in 2011 (see Ref. 8). All used electrodes can be sources of fluctuations and can lead to undesired errors. The solution of this problem is to exclude the gates at least partially, for example, to refuse electrodes controlling the exchange interaction and to find a way of the coupling control without electrodes.

There are some works where authors proposed quantum computation schemes based on the constant exchange coupling. The exchange coupling was eliminated by using encoded bits [9, 10], where two physical qubits in the states $\uparrow$ and $\downarrow$ are unified in one logical qubit $\uparrow\downarrow$. This configuration provides compensation of interactions with the environment. But two-qubit operations demand leaving the interaction-free space. By a strong local magnetic field the state $\uparrow\downarrow$ transforms to $\uparrow\uparrow$, and the interaction between logical qubits becomes switched on [9]. After performing the two-qubit operation the qubits are driven back to the interaction-free space. One more approach for elimination of the exchange interaction is based on refocusing pulses that are used in nuclear magnetic resonance (NMR) technique [Sec. 7.7.3 in Ref. 11]. It is applicable if the inter-qubit interaction Hamiltonian is diagonal in the computational basis. The repetition of refocusing pulses allows to suppress the interaction between qubits. Refocusing requires very fast repeated switchings with a period much shorter than the elementary operation time, that is quite difficult to implement in practice. Another complexity is locality of refocusing pulses, it requires injecting pulses onto every qubit of the quantum system. The use of strong local magnetic fields or the refocusing technique requires a more complicated architecture of the quantum computer, and we have a goal to find another way to eliminate the coupling

* nenashev@isp.nsc.ru

between qubits.

An idea proposed in the present work is close to the one of the work of Ozhigov and Fedichkin, [12] where elimination of the exchange interaction by all-the-time repetition of one-qubit operations was proposed. We offer repeating single-spin rotations for suppression of the exchange interaction, when the latter must be switched off. Our approach allows not only elimination of the exchange interaction, but also implementation of all basic logical operations.

This paper is organized as follows. In Sec. I we describe the intuitive scheme of our proposal, that is represented as a mathematical model in Sec. II. In Sec. III the ways of implementation of basic logical operations are discussed in the frame of this model. In Sec. IV the possibility of one- and two-qubit operations implementation is demonstrated by means of numerical experiments. The evolution of qubit states is found using the algorithms of the optimal control theory [13]. Optimization was performed using a combination of nonlocal search methods and a local descent by conjugate gradient methods.

I. MAIN IDEA

The intuitive scheme of our proposal is the following. We take two electrons with a constant exchange coupling between them and provide all-the-time rotation of their spins by application of the resonance microwave frequency radiation. These spin rotations eliminate the exchange interaction between electrons. For two-qubit gates implementation we switch on the exchange coupling taking electrons out of resonance. This can be done by simple addition of a small magnetic field $B \pm \delta B(t)$. The most important two-qubit operation CNOT can be done through the combination of single spin rotations and the $\sqrt{SWAP}$ operation. For the single-spin rotations electrons are driven to the resonance, and for the $\sqrt{SWAP}$ operation electrons are taken out of the resonance. Single spin rotations (when one electron spin of the coupled pair rotates, and the second one does not rotate) need the difference in electron g-factors. If this difference would be not so large (for example, $\delta g \sim 10^{-3}$) one can perform quantum operations by a small addition to the magnetic field $\delta B(t) \sim 1$ G, that can be produced by conventional coils used in NMR technique [14]. Such a difference δg can be realized by g-factor engineering in various quantum dot or quantum well systems, by changing the alloy composition in A_3B_5 [15, 16], or due to localization of electrons in different energetic valleys in a Ge/Si QD system [17]. A Ge/Si system with quantum dots seems to be more suitable, because such a pair of electrons can be localized at one quantum dot, one at the apex of the quantum dot, and a second electron at the QD base edge [17].

The essential difference of our approach from previous schemes of quantum computation is the use of the g-factor difference of two electrons for effective control (switching on/off) of the exchange interaction between them. In existing works the g-factor difference is used for addressing individual qubits and implementation of single-qubit operations. There have been proposed very original schemes of single-qubit gate implementation, using the g-factor difference, but without conventional microwave pulses [18, 19]. For example, in the work of Levy [18] periodic modulation of the exchange coupling within logical qubit at the Rabi frequency $\Omega = \Delta g B$ is proposed to produce π and $\pi/2$ pulses. In some works the g-factor difference is used in spin-charge conversion schemes. For example, in the work of Yokoshi *et al.* [20] sequential spin-to-charge conversions allow to implement the full Bell state measurement of electron-spin qubits. However, in all these proposals the exchange coupling must be controlled by electrodes. Our approach allows the implementation of single-qubit and two-qubit gates without electrodes controlling the exchange within one operational unit (an electron pair localized at one QD).

For large-scale quantum computation at least 1000 qubits are needed. It is possible to create a large ordered array of quantum dots by epitaxial growth on prepatterned substrates [21]. Let each quantum dot possess a pair of electrons with a constant coupling and different g-factors [17], then it can be considered as a basic element for logical gates implementation. Between quantum dots one can organize the $SWAP$ operations by means of additional electrodes created on the surface. Since all quantum dots are grown in one and the same growth manner, they are almost identical. To provide the selective access to an individual QD we suggest creating a parallel layer of smaller QDs (a storage layer), where two small quantum dots correspond to one large QD in the first layer (Fig. 1). Let electrons localized on smaller QDs have the g-factor quite different from g-factors of electrons in the first layer, then they are always out of resonance, and these quantum dots can serve as storage elements for electron spins. In the idle mode electrons are located in the storage layer. The similar structures were created using the strain-induced nucleation of QD molecules above buried nanomounds [22]. For performing logic gates the electrons from a pair of QDs in the storage layer are pushed to the corresponding QD in the upper (operation) layer by the "Address" electrode placed above the selected QD (see Fig. 1). The similar idea is described in Ref. 7 where electrons are driven by electrodes away from the dopant ion into layers of different alloy composition (and respectively different g-factors) for implementation of one- and two-qubit operations.

Our approach has the following advantages: it allows (i) to remove a half of electrodes controlling the exchange interaction, namely the electrodes controlling the exchange within electron pairs, (ii) to refuse the microwave pulse technics, (iii) to refuse the local strong magnetic field, because both magnetic fields B and $\delta B(t)$ used in our approach are global, (iv) to use standard ESR and NMR techniques.

In this work we verify the possibility of implementation

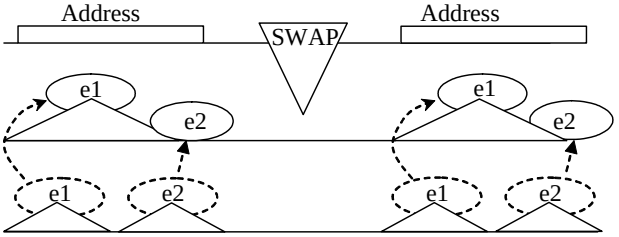

FIG. 1. Arrangement of quantum dots in the active (upper) layer and the storage (lower) layer, designed to perform quantum logic operations based on the control of the exchange interaction by means of the single spin rotations.

of basic logical operations on the example of the Ge/Si system with quantum dots. Ge QDs grown at certain growth conditions allow to localize two electrons on the same QD: near the QD apex and near the QD base edge (Fig. 1), that provides different g-factors due to localization in different Δ valleys, namely $g_{||} = 1.9995$ and $g_{\perp} = 1.9984$ [17]. Being close to each other, these electrons can have a sufficient overlap of wave functions required for two-qubit operations. One more advantage of the Ge/Si heterosystem is the location of electrons in Si, that can lead to long spin relaxation times due to small spin-orbit interaction in this material and small concentration of the ^{29}Si isotope with a nonzero nuclear spin [23, 24]. Direct measurements of electron spin lifetimes in dense arrays of Ge/Si QDs give the times of the order of 10 μs [25]. The spin lifetimes can be increased by switching off the main mechanism of spin relaxation in Ge/Si QD system—stochastic spin precession at the tunneling between QDs [26]. Indeed, partial suppression of the tunneling provides fourfold increase of spin lifetimes [27]. Further increase of spin lifetimes can be reached by using the isotopically pure material ^{28}Si [28]. In general, other heterosystems, such as A_3B_5, can be used for realization of our proposal.

II. MODEL

Let us represent the proposed model in a mathematical form. We consider two electrons with a constant tunneling coupling in the magnetic field (see Fig. 2). Let these electrons have close g-factors, differing on the small magnitude, $g_1 = g_0 - \delta g/2$ and $g_2 = g_0 + \delta g/2$ with $\delta g \ll g_0$. A constant magnetic field B_0 is applied in the z-direction, providing Larmor precession of the electron spins. This precession is described by the term

$$\hat{H}_0 = \mu_B B_0 (g_1 \hat{S}_{1z} + g_2 \hat{S}_{2z}),$$

where μ_B is the Bohr magneton, g_1 and g_2 are g-factors of the electrons, $\hat{\mathbf{S}}_1$ and $\hat{\mathbf{S}}_2$ are their spin operators.

Electrons are subjected to a microwave radiation circularly polarized in the xy-plane. The magnetic field $\mathbf{B}_w(t)$ of the microwave is

$$\mathbf{B}_m(t) = (B_{m_0} \cos \Omega t, B_{m_0} \sin \Omega t, 0),$$

where B_m is the amplitude of the microwave field, and Ω is the frequency. The latter is chosen to be equal to the mean value of Larmor frequencies of two electrons:

$$\hbar\Omega = \frac{g_1 + g_2}{2} \mu_B B_0,$$

thus both electrons in the stationary conditions are out of the spin resonance. The corresponding term in the Hamiltonian is

$$\hat{H}_m(t) = \mu_B \mathbf{B}_m(t)(g_1 \hat{\mathbf{S}}_1 + g_2 \hat{\mathbf{S}}_2).$$

These electron spins are considered as qubits. The model includes the interaction between qubits having a form of the Heisenberg exchange interaction:

$$\hat{H}_{int} = J \hat{\mathbf{S}}_1 \hat{\mathbf{S}}_2,$$

where J is the exchange integral, which is supposed to be constant.

The main idea is to make the system controllable with an addition of a small time-dependent magnetic field $\delta B(t)$. This magnetic field is also directed along the axis z, and the corresponding term in the Hamiltonian is

$$\hat{H}_c(t) = \mu_B \delta B(t)(g_1 \hat{S}_{1z} + g_2 \hat{S}_{2z}).$$

By means of this small additive it is possible to enter one of electrons into the resonance for a required time, and to carry out the spin turning on a desired angle through Rabi oscillations. Changing the additive $\delta B(t)$ one can rotate the spin of another electron. In this way it is possible to manipulate with qubits in this system and to carry out the main quantum logical operations.

The spin behavior becomes simpler in the reference frame, rotating with the frequency Ω. In this frame, the main contribution to the spin precession is removed and only relatively slow dynamics remains. The full Hamiltonian of the system of two coupled electrons, written in the rotating frame, takes the following form:

$$\hat{H}(t) = \hat{H}_0 + \hat{H}_m(0) + \hat{H}_{int} + \hat{H}_c(t) - \hbar\Omega(\hat{S}_{1z} + \hat{S}_{2z}).$$

In the basis $|\uparrow\uparrow\rangle$, $|\uparrow\downarrow\rangle$, $|\downarrow\uparrow\rangle$, $|\downarrow\downarrow\rangle$ this Hamiltonian has the following matrix representation:

$$\hat{H}(t) = \begin{pmatrix} \frac{J}{4} + g_0\mu_B\delta B(t) & \frac{g_0-\delta g/2}{2}\mu_B B_m & \frac{g_0+\delta g/2}{2}\mu_B B_m & 0 \\ \frac{g_0-\delta g/2}{2}\mu_B B_m & -\frac{J}{4} + \delta g(\frac{\hbar\Omega}{2g_0} + \frac{\mu_B\delta B(t)}{2}) & \frac{J}{2} & \frac{g_0+\delta g/2}{2}\mu_B B_m \\ \frac{g_0+\delta g/2}{2}\mu_B B_m & \frac{J}{2} & -\frac{J}{4} - \delta g(\frac{\hbar\Omega}{2g_0} + \frac{\mu_B\delta B(t)}{2}) & \frac{g_0-\delta g/2}{2}\mu_B B_m \\ 0 & \frac{g_0+\delta g/2}{2}\mu_B B_m & \frac{g_0-\delta g/2}{2}\mu_B B_m & \frac{J}{4} - g_0\mu_B\delta B(t) \end{pmatrix}. \quad (1)$$

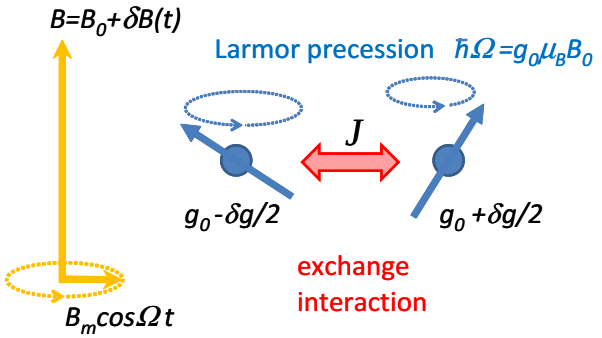

FIG. 2. The proposed model of the two-qubit system allowing the implementation of basic one- and two-qubit operations using a time-dependent global magnetic field $B(t)$.

III. REALIZATION

In this Section we describe the strategy for finding an appropriate control function $\delta B(t)$ for realization of desired one- or two-qubit operations. All operations are considered in the reference frame rotating with the frequency Ω around axis Z.

Let us introduce an "ideal" unitary operator $\mathbb{U}$ that is defined by the desired logical operation and transforms an initial state $|\psi_0\rangle$ of the system of two spins into a final state $\mathbb{U}|\psi_0\rangle$.

The actual evolution of the system state vector $|\psi_t\rangle$ is described by the equation

$$i\hbar\frac{d|\psi_t\rangle}{dt} = \hat{H}(t)|\psi_t\rangle, \quad (2)$$

where the Hamiltonian $\hat{H}(t)$ depends on $\delta B(t)$ according to Eq.(1). An unitary operator $\hat{U}_t$, that transforms $|\psi_0\rangle$ into $|\psi_t\rangle$, is defined by the equation

$$i\hbar\frac{dU_t}{dt} = \hat{H}(t)U_t, \quad (3)$$

and the initial condition that U_0 is the identity operator.

At some time T, the transformation $\hat{U}_{t=T}$ should become equivalent to the "ideal" operator $\mathbb{U}$, in order to perform desired logical operation without an error. In other words, for all $|\psi\rangle$ the results of actions of $\hat{U}_{t=T}$ and $\mathbb{U}$ should be physically equivalent:

$$U_{t=T}|\psi\rangle = \mathbb{U}|\psi\rangle\, e^{i\alpha}$$

with an arbitrary phase α. Then the transformations themselves are related in a similar way:

$$U_{t=T} = \mathbb{U}\, e^{i\alpha}.$$

The transformation $U_{t=T}$ depends on the function $\delta B(t)$ and on the duration T of the logical operation. To find the best implementation of the given quantum gate $\mathbb{U}$, we minimize the Frobenius norm of the deviation $\|U_{t=T} - \mathbb{U}\, e^{i\alpha}\|$ by variation of the function $\delta B(t)$ and parameters T and α.

The most suitable form of the small additive $\delta B(t)$ is

$$\delta B(t) = A\cos(\omega t + \varphi) + C \quad (4)$$

with parameters A, ω, φ, C depending on the type of the desired logical operation. Such dependence can be easily realized experimentally. Changing these parameters, one can perform various one- and two-qubit quantum gates, as it will be demonstrated below.

Fig. 3 demonstrates the example of behavior of error functional

$$f(t) = \min_\alpha \|U_t - \mathbb{U}\, e^{i\alpha}\|^2, \quad (5)$$

during the operation "$\pi/2$-rotation around Z". It is clearly seen that the error functional has the minimum value at $t = T$.

One can also use a more complicated modulated function $\delta B(t)$ having zero values at the beginning and at the end of the control action:

$$\delta B(t) = A\sin(\omega_0 t)(\cos(\omega t + \varphi) + C), \quad (6)$$

where $\omega_0 = 2\pi/T$ with T being the time of gate implementation. Such a form of the control function is convenient from the standpoint of the implementation of a large sequence of logical operations and smooth interfacing between operations. The search for optimal parameters (ω_0, A, ω, φ, C) of the function (6) can be done in two stages. The first step is the solution of the problem with a control function described by Eq. (4) to determine the time T at which the error of gate implementation is minimal. At the second step one can apply the function described by Eq. (6) with $\omega_0 = 2\pi/T$ to refine the solution.

In the following Section we will demonstrate that at reasonable values of tunneling coupling and g-factor difference one can realize a minimal set of one- and two-qubit operations required for quantum computation. As

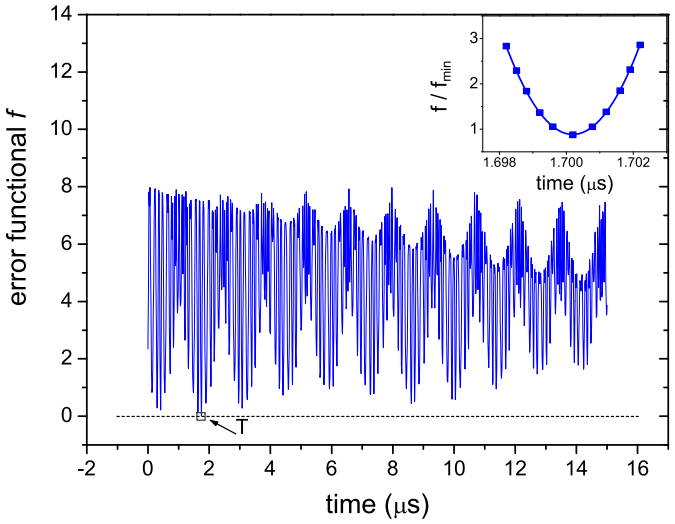

FIG. 3. Time dependence of the error functional $f(t)$, Eq.(5), for the operation "$\pi/2$-rotation around Z". The time, when the error functional has the minimum, is indicated as T. Inset shows the tolerance range for the time T. One can see that the end of logical gate can be controlled with accuracy ± 2 ns, at that the increase of error f does not exceed threshold $3f_{min}$.

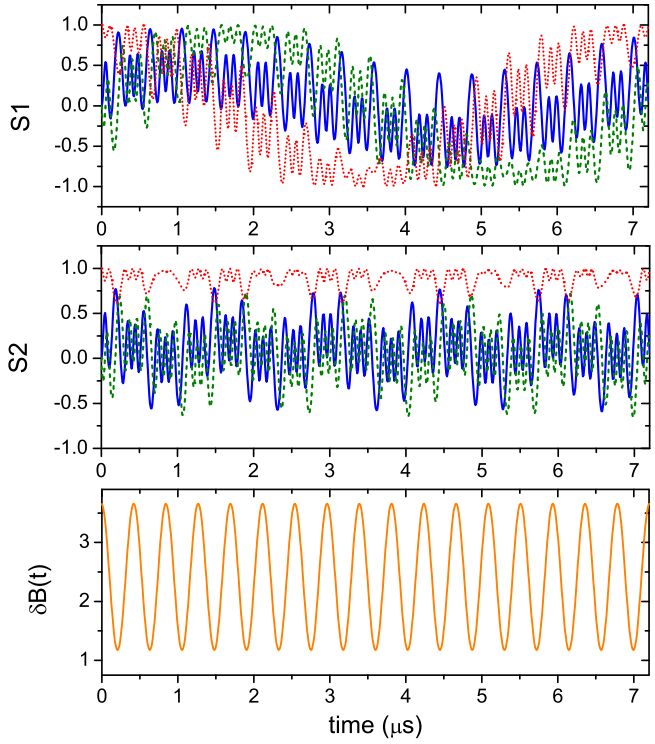

FIG. 4. Time evolution of spin components of the first (top panel) and the second electron (center panel) during "Storage operation". The blue solid curves are related to the S_x-components of the electron spins $\mathbf{S}_1$ and $\mathbf{S}_2$, the green dashed curves are related to the S_y-components, the red dotted curves are related to the S_z-components. The control magnetic field $\delta B(t)$ is shown in the bottom panel.

we mentioned above, the small difference of g-factors $\delta g \sim 10^{-3}$ observed recently in Ge/Si system with quantum dots [17] is suitable for our purposes. The magnitude of the exchange interaction can be estimated as $J \sim 4I^2/U \sim 10^{-10}$ eV, where I is the tunneling integral, $I \sim 10^{-3}$ meV, and U is the Coulomb interaction, $U \sim 30$ meV. The microwave magnetic field can be taken as $B_m = 1$ G. The time-dependent magnetic fields create the electric fields, but their magnitude is rather small. The alternating magnetic field with an amplitude ~ 1 G causes the electric field of the order of 300 V/cm. On the quantum dot length scale (~ 10 nm) the induced voltage is about 0.3 mV. Compared with the electron confinement potential in QD system (~ 100 meV), this value is negligible, and we do not take its effect into account.

IV. RESULTS AND DISCUSSION

In Table I the time T and the value of gate fidelity F are given for all verified logical operations. The gate fidelity is the probability of obtaining the correct result, averaged over all initial states [3, 29]. The connection between the error functional f and fidelity F is described in Appendix A. For all realizations we use the function $\delta B(t)$ described by Eq.(4). Parameters A, ω, φ, C were chosen to minimize the deviation of the fidelity from 1, using the optimization methods described in Ref. 12.

Fig. 4 demonstrates the results for the operation "quantum information storage". The top panel shows the evolution of spin components S_x, S_y, S_z for the first electron. For the second electron the spin evolution is shown at the central panel. And the bottom panel demonstrates the time dependence of the magnetic field $\delta B(t)$, that provides the conservation of the system in the initial state. It is clearly seen that the system under the action of the controlling magnetic field returns to its initial state. The different behavior is observed for the first and the second electrons, the first electron besides high-frequency oscillations of spin components has low-frequency ones, while the second electron has only high-frequency oscillations. This difference is explained by nonzero constant C in the function $\delta B(t)$, that shifts one of the electrons closer to the resonance. In principle, it is possible to realize the identical behavior of the spins with $C = 0$, certainly in this case the time T and other parameters of the function $\delta B(t)$ will be changed.

In Fig. 5 the evolution of the electron spins without time-dependent controlling magnetic field is shown. Results demonstrate that it is impossible to find such a moment of time, at which both electron spins return to their initial orientations.

The evolution of electron spins for the operation "$\pi/2$-rotation around Z" is presented in Fig. 6 for the following initial conditions. The first electron spin is oriented along the axis X, the second electron spin is directed along axis Z. As a result of the operation, the spin of

TABLE I. Results of numerical experiments. The controlling magnetic field has the form $\delta B(t) = A\cos(\omega t + \varphi) + C$. The value $(1 - F)$ gives the averaged probability of the error, F is the gate fidelity. The results were obtained for the following parameters: mean g-factor value $g_0 = 2$, g-factor difference $\delta g = 1.1 \cdot 10^{-3}$, exchange interaction $J = 10^{-10}$ eV, microwave frequency $\Omega = 9 \cdot 10^9$ Hz, microwave field amplitude $B_m = 1$ G.

Operation	$1 - F$	ω (MHz)	A (G)	φ	C (G)	$T(\mu s)$
Storage	$1.95 \cdot 10^{-5}$	14.80	1.24	0.08	2.417	7.212
$\sqrt{SWAP}$	$9.44 \cdot 10^{-4}$	6.79	0.99	3.14	−0.009	11.104
$SWAP$	$1.06 \cdot 10^{-3}$	6.79	0.87	0.00	−0.005	22.209
$\pi/2$-rotation around Z	$4.00 \cdot 10^{-3}$	14.39	0.81	0.85	2.319	1.700
$\pi/2$-rotation around X	$3.64 \cdot 10^{-3}$	17.43	1.96	6.27	−2.710	9.375
$\pi/2$-rotation around Y	$4.53 \cdot 10^{-3}$	14.40	1.24	1.82	1.323	1.309
$\pi/4$-rotation around X	$1.40 \cdot 10^{-3}$	9.741	0.07	3.05	0.253	0.664
$\pi/8$-rotation around X	$5.55 \cdot 10^{-3}$	4.816	1.00	5.99	−0.029	1.424

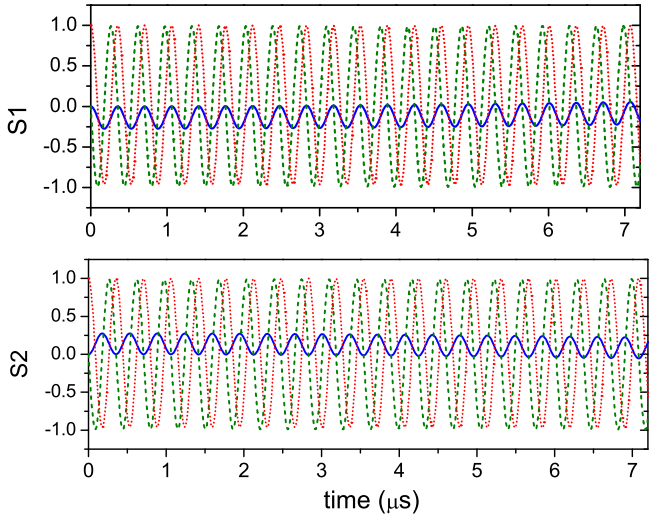

FIG. 5. Free evolution of spin components ($\delta B = 0$) of the first (top panel) and the second electron (bottom panel). The system does not return to the initial state.

the first electron has arrived to the orientation along the axis Y, while the second electron spin has returned to its initial orientation. This demonstrates the correctness of the proposed gate implementation.

Fig. 7 demonstrates the system evolution for the $SWAP$ operation. This operation is implemented if the initial state transforms to the final state in the following manner:

$$|\uparrow\uparrow\rangle \to |\uparrow\uparrow\rangle\, e^{i\alpha},$$
$$|\uparrow\downarrow\rangle \to |\downarrow\uparrow\rangle\, e^{i\alpha},$$
$$|\downarrow\uparrow\rangle \to |\uparrow\downarrow\rangle\, e^{i\alpha},$$
$$|\downarrow\downarrow\rangle \to |\downarrow\downarrow\rangle\, e^{i\alpha},$$

where horizontal arrows represent the transformation from $|\psi_0\rangle$ to $|\psi_T\rangle$ under the given Hamiltonian. In Fig. 7 the first electron was initially in the spin-down state, and the second one was in the spin-up state. As result of operation the electrons have exchanged their spin directions.

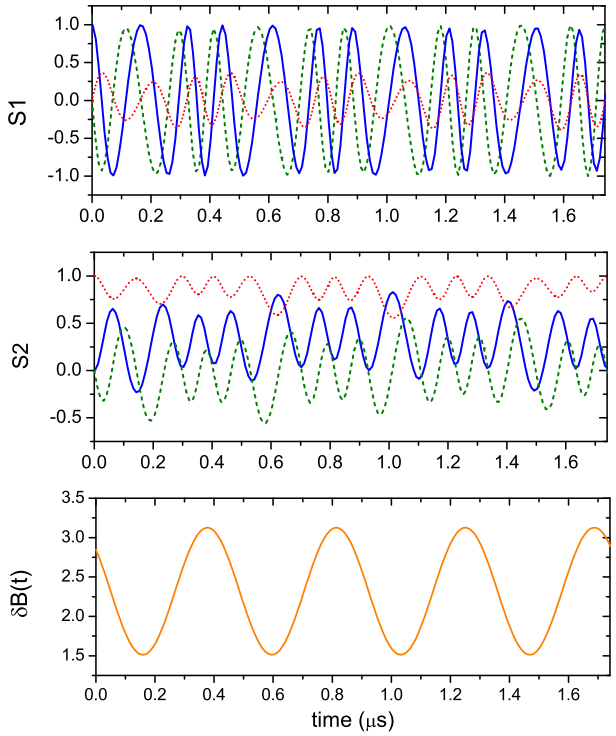

FIG. 6. Time evolution of the spin components of the first (top panel) and the second electron (center panel) during the operation "$\pi/2$-rotation around Z". The blue solid curves are related to S_x-components of electron spins $\mathbf{S}_1$ and $\mathbf{S}_2$, the green dashed curves are related to S_y-components, the red dotted curves are related to S_z-components. The control magnetic field $\delta B(t)$ is shown in the bottom panel.

Simple reduction of the operation time by a factor of 2, $T = T_{SWAP}/2$, produces the $\sqrt{SWAP}$ gate, which has then the maximum entangling capability. The results presented in Table I show that the frequency ω is the same for the $\sqrt{SWAP}$ and $SWAP$ gates, when the amplitude A and the phase φ are slightly different.

The error probability $(1-F)$ for the spin rotation gates is found in the range $(1.4 \div 5.5) \cdot 10^{-3}$, while the error probability for the $SWAP$ operation is approximately

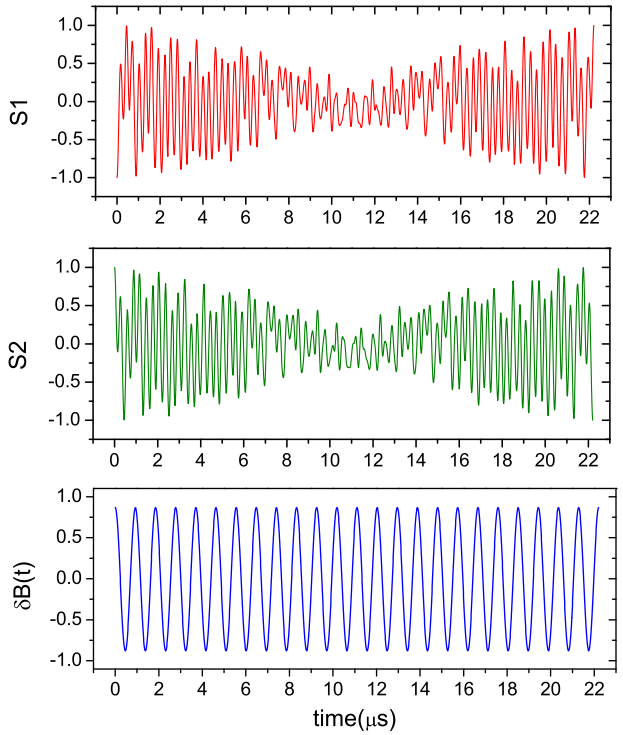

FIG. 7. Time evolution of S_z-components of the first (top panel) and the second electron (center panel) during the $SWAP$ operation. The control magnetic field $\delta B(t)$ is shown in the bottom panel.

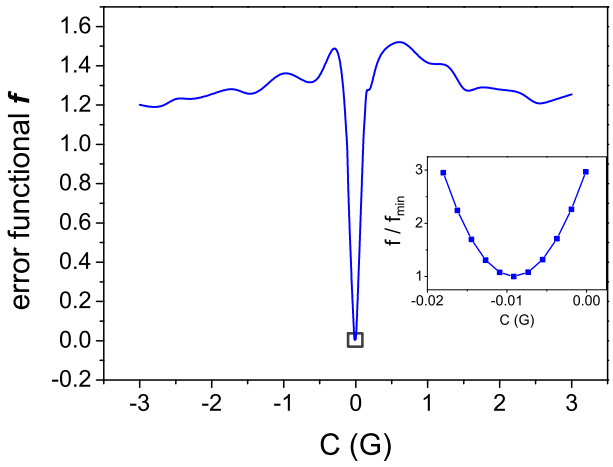

FIG. 8. Dependence of the error functional f on the deviation of the parameter C (a constant shift in the controlling field $\delta B(t) = A\cos(\omega t + \varphi) + C$) for the $\sqrt{SWAP}$ gate. Inset shows that at $\Delta C \leq 0.01$ G the error f does not exceed the threshold $3f_{min}$.

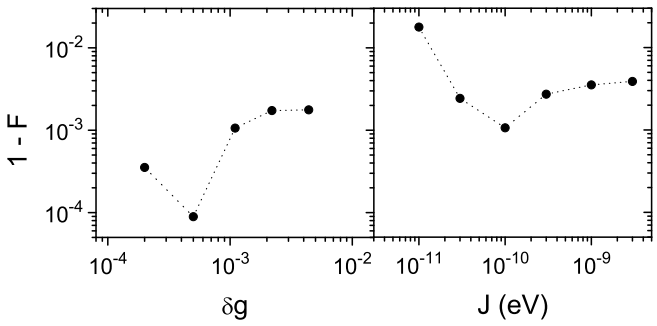

FIG. 9. Dependence of the error $(1-F)$ on the g-factor difference δg (left panel) and on the exchange integral J (right panel) for the $SWAP$ gate. Here F is the gate fidelity.

10^{-3}. We suppose that the main source of errors in single qubit operations (spin rotations) is a closeness of electron g-factors. To verify this hypothesis we perform numerical experiments for the operation "$\pi/2$-rotation around X" with twofold increased $\delta g = 2.2 \cdot 10^{-3}$. As a result we obtain the five-fold reduction of the error, $(1-F) \approx 10^{-3}$.

A quality of the $SWAP$ operation depends on two parameters: exchange interaction J and detuning $\delta g/2$ of the electron g-factors from the resonance. If the magnitude of the exchange will be very large, the evolution of the two-electron system becomes less controllable. For example, the numerical experiment for the $SWAP$ gate with $J = 10^{-9}$ eV (at $\delta g = 1.1 \cdot 10^{-3}$) gives the error $(1-F) = 3.52 \cdot 10^{-3}$. Regarding the parameter δg, its increase also leads to the error rise. In particular, the $SWAP$ operation with $\delta g = 2.2 \cdot 10^{-3}$ ($J = 10^{-10}$ eV) has the error $(1-F) = 1.73 \cdot 10^{-3}$. In the last case the detuning of electrons from resonance is too strong and it becomes hard to use the spin rotations for control (or elimination) of the exchange interaction. In Fig. 9 the behavior of the error $(1-F)$ with change of δg and J is shown for the $SWAP$ operation. It is clearly visible that the values of $\delta g = 1.1 \cdot 10^{-3}$ and $J = 10^{-10}$ eV used in our numerical experiments are close to the optimal ones. It should be noted that we chose these values based on the parameters of real Ge/Si quantum dots. From the dependence shown in the left panel of Fig. 9 it seems that the value $\delta g = 5 \cdot 10^{-4}$ is more appropriate than $\delta g = 1.1 \cdot 10^{-3}$. However, the decrease of δg complicates the addressing individual qubits, that provokes the rise of the error $(1-F)$ during single-qubit operations. Thus, the search for the optimal values of δg and J should be carried out with respect to the whole set of one- and two-qubit operations.

It is worth noting that each optimization problem considered in this paper can have a few possible solutions with approximately equal errors. In principle one can use any of these solutions. Each solution has its own unique moment of time, when the system reaches the desired state. Since the behavior of the error functional f represents very strong oscillations, the success of our approach depends on the accuracy of time determination. The tolerable error Δt, at that the averaged probability of error $(1-F)$ stays the same order of magnitude, is about ± 2 ns (Fig. 3). Therefore the gate duration should be controlled with accuracy $\simeq 1$ ns. Such a requirement can be easily satisfied with modern experimental equip-

ment.

Additionally we have studied the reliability of our approach with respect to deviation of parameters of the controlling field $\delta B(t)$ (A, ω, ϕ, C) from their optimal values. The study was performed for the $\sqrt{SWAP}$ operation. In a real experiment all these parameters can be controlled with some accuracy, and we have found for each parameter the tolerance range at which the fidelity F remains of the same order as the optimal value. We define the tolerance range from the condition $f \leq 3f_{min}$, where f_{min} is the error functional value given in Table I. In Fig. 8 the tolerance range for the parameter C is shown. From the inset to this figure one can see that the tolerance range $\Delta C = \pm 0.01$ G. However, the fidelity is more sensitive to the amplitude A. The deviation $\Delta A = \pm 0.001$ G causes the increase of the error f up to $3f_{min}$. The frequency ω must be controlled with accuracy $\Delta\omega = \pm 5$ kHz. The tolerant change of the phase φ is $\Delta\varphi = \pm 0.12$. It should be noted that within the indicated tolerance ranges the time of the gate implementation does not change.

Finally we would like to discuss the experimental feasibility of the magnetic field control with required accuracy. The magnetic field in our proposal consists of two parts $B + \delta B(t)$. The first large part is of the order of 10^3 G, the second small part is about 1 G. Both fields should be stabilized with accuracy 10^{-3} G. The most challenging problem is stabilization of the large magnetic field, because the relative accuracy should be of the order of 10^{-6}. Modern superconducting magnets are able to meet this requirement. For example, the specification of uniformity of the magnetic fields in the general NMR apparatus is 0.01 ppm in a sample space and 0.01 ppm/hour in time-based stability. The additive part $\delta B(t)$ can be produced by a small extra coil, and should be controlled with a reasonable accuracy $\sim 0.1\%$.

V. CONCLUSIONS

We have proposed a new method of the implementation of one- and two-qubit gates in a system of two electrons with constant exchange coupling. The only controlled parameter is the small time-dependent addition to the magnetic field. Small g-factor difference between two electrons provides not only the selective access to the individual qubits, but also the effective control of the exchange interaction between them. We have verified the possibility of basic one- and two-qubit operations in the frame of proposed model and found the parameters of controlling magnetic field allowing to perform these operations with an acceptable accuracy.

ACKNOWLEDGMENTS

This work was supported by RFBR (Grant 13-02-12105), SB RAS integration project No. 83 and DITCS RAS project No. 2.5.

Appendix A: relation between error functional and fidelity

In this Appendix, we will show how to find the gate fidelity F from the functional f defined by Eq. (5).

Frobenius norm of a square matrix A is defined as

$$\|A\| = \sqrt{\mathrm{Tr}\,(AA^+)},$$

therefore

$$\begin{aligned}\left\|U_t - \mathbb{U}\,e^{i\alpha}\right\|^2 &= \mathrm{Tr}\left[\left(U_t - \mathbb{U}\,e^{i\alpha}\right)\left(U_t^+ - \mathbb{U}^+\,e^{-i\alpha}\right)\right] \\ &= \mathrm{Tr}\left(U_t U_t^+\right) + \mathrm{Tr}\left(\mathbb{U}\mathbb{U}^+\right) - 2\,\mathrm{Re}\left[e^{i\alpha}\,\mathrm{Tr}\left(U_t^+\mathbb{U}\right)\right].\end{aligned}$$

In the latter expression, $U_t U_t^+$ and $\mathbb{U}\mathbb{U}^+$ are identity matrices 4×4, so their traces are equal to 4. Denoting the remaining trace as Z,

$$Z = \mathrm{Tr}\left(U_t^+\mathbb{U}\right),$$

one obtains the following relation:

$$\left\|U_t - \mathbb{U}\,e^{i\alpha}\right\|^2 = 8 - 2\,\mathrm{Re}\left(e^{i\alpha}\,Z\right).$$

Hence, according to Eq. (5),

$$f(t) = \min_\alpha \left\|U_t - \mathbb{U}\,e^{i\alpha}\right\|^2 = 8 - 2\,|Z|. \qquad \text{(A1)}$$

Since the matrix $U_t^+\mathbb{U}$ is unitary, its four eigenvalues can be expressed as $e^{i\varphi_1}, \ldots, e^{i\varphi_4}$, where $\varphi_1, \ldots, \varphi_4$ are real numbers. So the trace Z of this matrix is equal to

$$Z = \sum_{k=1}^{4} e^{i\varphi_k},$$

therefore

$$\begin{aligned}|Z|^2 &= \sum_k \sum_l e^{i\varphi_k} e^{-i\varphi_l} \\ &= 4 + 2\sum_{k<l} \cos(\varphi_k - \varphi_l) \equiv 4 + 2M, \qquad \text{(A2)}\end{aligned}$$

where

$$M = \sum_{k<l} \cos(\varphi_k - \varphi_l).$$

Using Eqs. (A1) and (A2), one can express the quantity f via M:

$$f = 8 - 2\sqrt{4 + 2M}. \qquad \text{(A3)}$$

Now let us express the gate fidelity F via M. The gate fidelity is the probability, averaged over all initial state vectors $|\psi\rangle$, that the system will be found in the desired state $\mathbb{U}|\psi\rangle$ after passing through the gate:

$$F = \overline{\left|\langle\psi|U_t^+\mathbb{U}|\psi\rangle\right|^2},$$

where the overline denotes averaging over initial states. Let us consider this expression in a basis that diagonalizes the matrix $U_t^+\mathbb{U}$:

$$U_t^+\mathbb{U} = \begin{pmatrix} e^{i\varphi_1} & 0 & 0 & 0 \\ 0 & e^{i\varphi_2} & 0 & 0 \\ 0 & 0 & e^{i\varphi_3} & 0 \\ 0 & 0 & 0 & e^{i\varphi_4} \end{pmatrix}, \quad |\psi\rangle = \begin{pmatrix} c_1 \\ c_2 \\ c_3 \\ c_4 \end{pmatrix},$$

where $c_1, \ldots, c_4$ are complex amplitudes that define the state $|\psi\rangle$. In this basis,

$$\langle\psi|U_t^+\mathbb{U}|\psi\rangle = \sum_{k=1}^{4} |c_k|^2 e^{i\varphi_k},$$

therefore

$$F = \sum_k \sum_l \overline{|c_k|^2|c_l|^2} e^{i\varphi_k} e^{-i\varphi_l} = \sum_k \overline{|c_k|^4} + 2\sum_{k<l} \overline{|c_k|^2|c_l|^2} \cos(\varphi_k - \varphi_l).$$

It is possible to show that

$$\overline{|c_k|^2|c_l|^2} = \begin{cases} 1/10 & \text{if } k = l, \\ 1/20 & \text{if } k \neq l, \end{cases}$$

therefore

$$F = \frac{4 + M}{10}. \tag{A4}$$

Comparing Eqs. (A3) and (A4), one can easily see that

$$F = 1 - \frac{f}{5}\left(1 - \frac{f}{16}\right). \tag{A5}$$

If f is small enough, then $(1 - F)$ is approximately proportional to f:

$$1 - F \approx \frac{f}{5}.$$

Hence, the minimization of the error functional f is equivalent to the minimization of the deviation of the fidelity F from 1.

[1] T. D. Ladd, F. Jelezko, R. Laflamme, Y. Nakamura, C. Monroe, and J. L. O'Brien, *Nature* **464**, 45 (2010).

[2] D. P. DiVincenzo, in *Mesoscopic Electron Transport*, eds. Sohn, Kowenhoven, Schoen (Kluwer 1997), p. 657, cond-mat/9612126; The Physical Implementation of Quantum Computation, Fort. der Physik **48**, 771 (2000), quant-ph/0002077

[3] D. Loss and D. P. DiVincenzo, Phys. Rev. A **57**, 120 (1998).

[4] L. P. Kouwenhoven, C. M. Marcus, P. L. McEuen, S. Tarucha, R. M. Westervelt and N. S. Wingreen. *Mesoscopic Electron Transport Series E*, ed. L. L. Sohn, L. P. Kouwenhoven and G. Schön (Dordrecht: Kluwer), **345**, 105 (1997).

[5] W. G. Van der Wiel, S. De Franceschi, J. M. Elzerman, T. Fujisawa, S. Tarucha and L. P. Kouwenhoven, Rev. Mod. Phys. **75** 1 (2003).

[6] H. A. Engel and D. Loss, Phys. Rev. Lett. **86**, 4648 (2001).

[7] R. Vrijen, E. Yablonovitch, K. Wang, H. W. Jiang, A. Balandin, V. Roychowdhury, T. Mor, D. DiVincenzo, Phys. Rev. A **62**, 012306 (2000).

[8] R. Brunner, Y.-S. Shin, T. Obata, M. Pioro-Ladriere, T. Kubo, K. Yoshida, T. Taniyama, Y. Tokura, and S. Tarucha, Phys. Rev. Lett. **107**, 146801 (2011).

[9] Y. Hu, Z.-W. Zhou, G.-C. Guo, New Journal of Physics **9**, 27 (2007).

[10] X. Zhou, Z.-W. Zhou, G.-C. Guo, and M. J. Feldman, Phys. Rev. Lett. **89**, 197903 (2002).

[11] M. A. Nielsen, I. L. Chuang *Quantum Computation and Quantum Information* (Cambridge University Press, New York, 2010).

[12] Y. Ozhigov, L. Fedichkin, JETP Letters **77**, 328 (2003).

[13] C.A. Floudas and P.M. Pardalos (Eds.), *Encyclopedia of Optimization* (Second edition, Springer, 2009).

[14] A. Abragam, *The principles of nuclear magnetism* (Oxford: Clarendon Press, 1961).

[15] E. L. Ivchenko and A. A. Kiselev, Sov. Phys. Semicond. **26**, 827 (1992).

[16] H. Kosaka, A. A. Kiselev, F. A. Baron, K. W. Kim, and E. Yablonovitch, Electron. Lett. **37**, 464 (2001).

[17] A. F. Zinovieva, A. I. Nikiforov, V.A. Timofeev, A. V. Nenashev, A. V. Dvurechenskii, L. V. Kulik, Phys. Rev. B **88**, 235308 (2013).

[18] J. Levy, Phys. Rev. Lett. **89**, 147902 (2002).

[19] J. M. Taylor, H.-A. Engel, , W. Duë, A. Yacoby, C. M. Marcus, P. Zoller, M. D. Lukin Nature Physics **1**, 177 (2005).

[20] N. Yokoshi, H. Imamura, H. Kosaka, Phys. Rev. B **81**, 161305 (2010).

[21] M. Grydlik, G. Langer, T. Fromherz, F. Schäffler, M. Brehm, Nanotechnology **24**, 105601 (2013).

[22] V. A. Zinovyev, A. V. Dvurechenskii, P. A. Kuchinskaya, and V. A. Armbrister, Phys. Rev. Lett. **111**, 265501 (2013).
[23] G. Feher, Phys. Rev. **114**, 1219 (1959); G. Feher and E. Gere, Phys. Rev. **114**, 1245 (1959).
[24] M. Chiba and A. Hirai, J. Phys. Soc. Jpn. **33**, 730 (1972).
[25] A. F. Zinovieva, A. V. Dvurechenskii, N. P. Stepina, A. I. Nikiforov, A. S. Lyubin, L. V. Kulik, Phys. Rev. B. **81**, 113303 (2010).
[26] A. F. Zinovieva, N. P. Stepina, A. I. Nikiforov, A. V. Nenashev, A. V. Dvurechenskii, L. V. Kulik, M. C. Carmo, and N. A. Sobolev, Phys. Rev. B **89**, 045305 (2014).
[27] A. F. Zinovieva, A. V. Nenashev, A. V. Dvurechenskii, Phys. Rev. B **71**, 033310 (2005).
[28] E. Abe, A. M. Tyryshkin, S. Tojo, J. J. L. Morton, W. M. Witzel, A. Fujimoto, J. W. Ager, E. E. Haller, J. Isoya, S. A. Lyon, M. L. W. Thewalt, K. M. Itoh, Phys. Rev. B **82**, 121201(R) (2010).
[29] J. F. Poyatos, J.-I. Cirac, and P. Zoller, Phys. Rev. Lett. **78**, 390 (1997).